



## QUASI 3D MODELING OF STREAMFLOW IN HYDRO POWER PLANTS DOWNSTREAM RESERVOIRS TO USE THE REMAINING ENERGY THROUGH HYDROKINETIC TURBINES

**Cleudson Alves da Silva**

**Claudio José Cavalcante Blanco**

Civil Engineering Graduate Program of the Federal University of Pará–PPGEC/ITEC/UFPA, Rua Augusto Corrêa 1, Belém, PA, 66075-110, Brazil

School of Environmental and Sanitary Engineering - FAESA/ITEC/UFPA, Rua Augusto Corrêa 1, Belém, PA, 66075-110, Brazil

cleudson.alves@itec.ufpa.br

blanco@ufpa.br

**André Luiz Amarante Mesquita**

Amazon Development Center in Engineering, Federal University of Pará – NIDAE/CAMTUC/UFPA, Av. Brasília, S/N - Vila

Permanente, Tucuruí, PA, 68455-901, Brazil

andream@ufpa.br

**Patrícia da Silva Holanda**

Graduate Program in Natural Resource Engineering in the Amazon of the Federal University of Pará–PRODERNA/ITEC/UFPA,

Rua Augusto Corrêa 1, Belém, PA, 66075-110, Brazil

pholanda@ufpa.br

**Nelio Moura de Figueiredo**

School of Naval Engineering FENAV/ITEC/UFPA, Rua Augusto Corrêa 1, Belém, PA, 66075-110, Brazil

nelio@ufpa.br

**Antonio Cesar Pinho Brasil Junior**

Faculty of Technology of Mechanical Engineering/UnB, Campus Universitário Darcy Ribeiro, CEP 70910-900, Brasília, DF, Brazil

brasiljr@unb.br

**Yves Secretan**

Institut National de la Recherche Scientifique–Eau, Terre Et Environnement-INRS-ETE/Université du Québec, 490, rue de la

Couronne, Québec, QC, G1K 9A9, Canada

yves.secretan@ete.inrs.ca

**Abstract.** *The demand for electricity to increase, as the population increases, and thus, the transformation of natural resources into durable and consumer goods increases. Therefore, there is a great need for electric power generation to sustain world economic growth. In this context, the use of the remaining energy due to the usable discharge and spilled flow into the reservoirs downstream of Hydro Power Plant (HPP) by hydrokinetic turbines is interesting. The objective of the paper is to develop a methodology for extrapolating velocities in transects of reservoirs downstream from HPP based on hydrodynamic fluvial modeling (Saint-Venant 2D model), resulting in Quasi 3D velocities profiles. In this case, bathymetry and topography data were extracted from satellite images. The hydrodynamic mesh and the solution of the Saint-Venant Equations were obtained using the Finite Element Method. The methodology have been applied to the Serra do Facão HPP downstream reservoir, Goiás, Brazil. Flow and water level data for the 2D model boundary conditions were made available by the National Electric System Operator. The Quasi 3D model was based on a logarithmic distribution profile, which models the vertical flow acceptably, according to classical literature. Velocity isosurfaces regions resulting from 2D modeling were selected due to the higher velocities, which maximize the generation of hydrokinetic energy, as they vary with the velocity cube. Thus, for two sections with higher velocities and maximum depths of 5 m, the maximum simulated velocity was equal to 2.5 m/s. With this velocity and taking half the depth for dimensioning the diameter of two hydrokinetic turbines, one for each section, there is a hydraulic power equal to 19.2 kW. This result is interesting, as hydrokinetic parks can be installed in the downstream reservoirs, increasing the potential found in the study.*

**Keywords:** *Quasi 3D model, remaining energy, logarithmic distribution, hydrokinetic turbines, finite element method*

## 1. INTRODUCTION

The greater the transformation of natural resources into durable goods, the greater the demand for electricity for the production and consumption of these goods. Therefore, what is observed is a great need for the generation of electric energy to sustain world economic growth. In this context, the use of remaining flows downstream of Hydro Power Plant (HPP) by hydrokinetic turbines is interesting. The technology of hydrokinetic power plants has been explored due to the energy conversion having a low environmental impact, thus favoring a gain in the generation of electric energy, taking into account, still, that the region is already impacted by the HPP (Holanda *et al.*, 2017). To take advantage of this energy source, the hydrodynamic modeling 1DH and 2DH are presented as computational tools to estimate the hydrokinetic potentials of these areas, aiming at simulating velocities and depths for the dimensioning of hydrokinetic plants.

Duvoy and Toniolo (2012) developed the CCHE2D, which is a 2DH type model for estimating hydrokinetic energy in rivers. The model was developed by the National Center for Computational Hydroscience and Engineering, University of Mississippi. The model outputs speeds, which are used by the Hydrokal (hydrokinetic calculator) to calculate the hydrokinetic power density. The model was applied to the Tanana River near Nenana, Alaska, USA. Punys *et al.* (2015) assessed the hydrokinetic potential of the Neris River, Lithuania, which is one of the largest rivers in the country. The authors used the 1DHEC-RAS model to simulate the river flow. The model was validated from a historical series of streamflow, velocity and transversal area data, in three calibration stations. Ramirez *et al.* (2016) conducted a study on the potential use of hydrokinetic turbines in the streamflow channels of HPPs in Colombia. They also used the 1DHEC-RAS model to obtain velocity and depth data in cross sections of the channels. The authors concluded that the use of hydrokinetic turbines in the streamflow channels of HPPs in the case studies presented is not recommended due to the financial infeasibility. Holanda *et al.* (2017) evaluated the hydrokinetic potential of the Tucuruí HPP downstream reservoir, using the Saint-Venant (2DH) model to simulate velocities and depths. The results showed that the Tocantins River channel has the highest velocities and depths, with the implantation of 10 hydrokinetic turbines, producing 2,04 GWh/ano. Guerra and Thomson (2019) analyzed the implementation of a large-scale hydrokinetic turbine in the Kvichak River (Alaska) in relation to streamflow modification. Thus, three dynamic regions were perceived, an induction zone, where velocities decrease and turbulence increases, a track, where reduced velocities recover slightly and high turbulence decays quickly, and a track well beyond the turbine, where reduced velocities are persistent and turbulence remains high. Santos *et al.* (2021) present a methodology for assessing the length of the rotor hydrokinetic wake in natural channels using CFD and the actuator disk model. These techniques were applied to a portion of the Amazon River. The wake length was between 7 and 9 diameters. The study of the hydrokinetic arrangement of three turbines was also carried out and an electrical power of 18,3 kW.

The objective of the article is to present a Quasi 3D model with a logarithmic profile determined with velocity and depth data obtained through the 2DH model (Holanda *et al.*, 2017). The quasi 3D model was applied to the downstream reservoir of HPP Serra do Facão located in the state of Goiás, Brazil. In this case, topobathymetry data were estimated through satellite images and streamflow and water level data from the national system operator (ONS) were used for streamflow simulations.

## 2. MATERIAL AND METHODS

### 2.1 Study area

The study area is the HPP Serra do Facão (Figure 1), located on the São Marcos River, in the state of Goiás (GO), Brazil, located 58 km from the city of Catalão and close to 27 km from the city of Davinópolis. The geographical coordinates are latitude 18° 04' South and longitude 47° 40' West (SEFAC, 2020). The HPP (Figure 1) has an installed power of 212,6 MW (two Francis-type turbines with 106,3 MW each, the diameter of the rotor is 4.160 mm, rotation of 171,4 rpm, number of rotor blades equal to 13 and number of distributor blades equal to 24). The installed power is 178,8 MW medium, which are sufficient to supply the energy demand of a city with approximately 1.2 million inhabitants (FURNAS, 2020). The HPP upstream reservoir has an area of 218,84 km<sup>2</sup> and bathes lands in the municipalities of Catalão, with 72.8%; Campo Alegre de Goiás, with 22.4%; Crystalline, with 0.6%; Davinópolis, with 0.4% and Ipameri, with 0.1%, in the state of Goiás, and Paracatu with 3.7%, in the state of Minas Gerais (SEFAC, 2020).

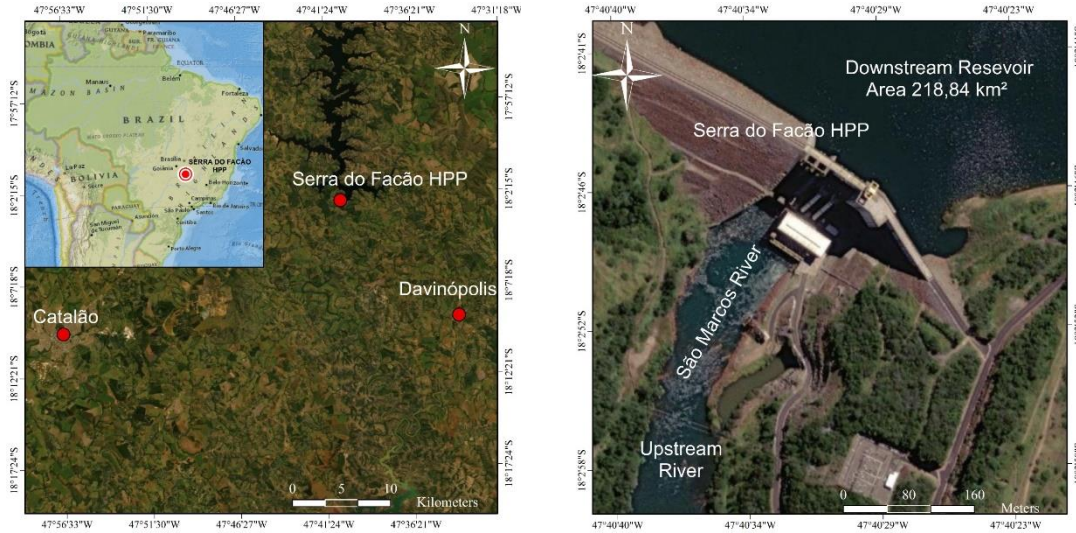


Figura 1. Location of the Serra do Facão HPP and the upstream and downstream reservoirs.

## 2.2 Batimetria via imagens de satélite

Estimates based on multispectral satellite images offer a good alternative for the extraction of topobathymetric data due to its low cost, relatively high spatial and temporal resolution and wide coverage (Geyman and Maloof, 2019). All algorithms for extracting water depth from satellite images are based on the physical principle that water refracts light. In general terms, bathymetric algorithms can be grouped into two categories: empirical methods, which use direct observations of the depth of water in the study area to calibrate the reflectance-depth relationship; and physics-based inversion algorithms that use radiative transfer models to calculate water depth (Kerr and Purkis, 2018).

Kerr and Purkis (2018) provide a bridge between empirical and physics-based approaches, coupling direct modeling of the water column (Lee *et al.*, 1999) with the Stumpf *et al.* (2003) proportion algorithm, which is widely applied in empirical studies. Although linear and ratio algorithms are unable to fully accommodate the various types of backgrounds, they are more likely to produce reasonable depth estimates for regions outside the range of calibration data, since linear and ratio algorithms are still substantiated by radiative transfer physics in seawater (Stumpf *et al.*, 2003). In this work, the ratio algorithm (Eq. (1)) was used, which is an attempt to derive a depth estimate independent of the reflectance base (Stumpf *et al.*, 2003).

$$z = m \frac{\log R(\lambda_i)}{\log R(\lambda_j)} + c_i, \quad (1)$$

Where  $z$  is the depth,  $R(\lambda_i)$  e  $R(\lambda_j)$  are the reflectances in the bands  $i$  and  $j$ , respectively and  $m$  and  $c_i$  are parameters used for calibration with data from the topography of the study area.

Equation 1 orthorectified satellite images were applied to the charts with information that follow the Terrestrial Systematic Topographic Mapping of Brazil with cartographic base on the scale of 1:250.000 - BC250 (IBGE, 2020).

## 2.3 Hydrodynamic Model

The hydrodynamic model adopted in this work is the longitudinal-transversal bidimensional, and the velocities  $v(x,y)$ , are averages in the direction  $z$  (Secretan and Leclerc, 1998). The equations of conservation of mass and conservation of the amount of movement were integrated along the depth in the vertical direction. Such integration is favored by the hypothesis that the gradients in the directions  $x$  and  $y$  are more important than the ones in the direction  $z$  (Figure 2). Thus, having the classic Saint-Venant model for shallow water, considering, still, other hypotheses (Saint-Venant, 1871; Heniche *et al.*, 2000).

- The water column is mixed in the vertical direction and the depth is small compared to the width and length of the river; and

- The waves are of small amplitude and of long period. The vertical acceleration component is insignificant, which allows the hydrostatic pressure to approach.

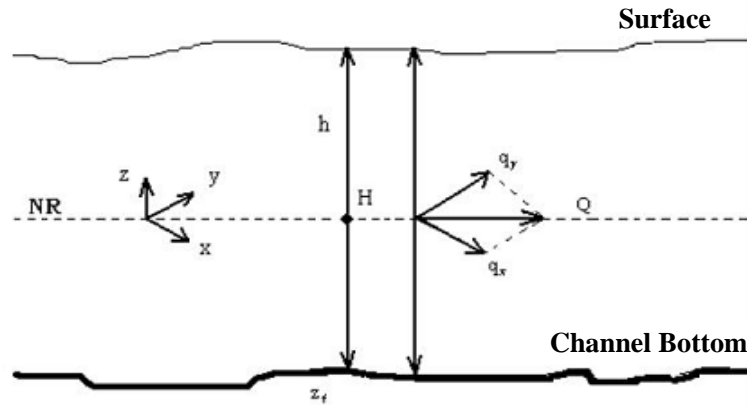


Figure 2. Coordinate system for vertically integrated equations.  
 Source: Secretan *et al.* (2000)

Adequacy of the Saint-Venant model for simulating the hydrodynamic behavior of the São Marcos river is justified by: absence of thermal stratification; small variations in salinity and vertical velocity components are also small. In this case, Eq. (2) is the mass conservation equation, while Eqs. (3) and (4) are the equations for the conservation of the amount of movement.

$$\frac{\partial h}{\partial t} + \frac{\partial q_x}{\partial x} + \frac{\partial q_y}{\partial y} = 0 \quad (2)$$

$$\frac{\partial q_x}{\partial t} + \frac{\partial q_x \frac{q_x}{H}}{\partial x} + \frac{\partial q_x \frac{q_y}{H}}{\partial y} = \sum F_x \quad (3)$$

$$\frac{\partial q_y}{\partial t} + \frac{\partial q_y \frac{q_x}{H}}{\partial x} + \frac{\partial q_y \frac{q_y}{H}}{\partial y} = \sum F_y \quad (4)$$

Where  $q_x$  and  $q_y$  ( $m^3/s$ ) are the flows in the Cartesian coordinates  $x$  and  $y$ ;  $t$  (s) is the time;  $h$  (m) is the water level;  $H$  (m) is the depth of the water column, and  $F_x$  and  $F_y$  (N) are the forces of volumes in the directions  $x$  and  $y$ . The terms on the right side of Eqs. (3) and (4) are given by Eqs. (5) and (6).

$$\sum F_x = -gH \frac{\partial h}{\partial x} - \frac{n^2 g |\vec{q}| q_x}{H^3} + \frac{1}{\rho} \left( \frac{\partial(H\tau_{xx})}{\partial x} \right) + \frac{1}{\rho} \left( \frac{\partial(H\tau_{xy})}{\partial y} \right) + F_{cx} + F_{wx} \quad (5)$$

$$\sum F_y = -gH \frac{\partial h}{\partial x} - \frac{n^2 g |\vec{q}| q_y}{H^3} + \frac{1}{\rho} \left( \frac{\partial(H\tau_{yx})}{\partial x} \right) + \frac{1}{\rho} \left( \frac{\partial(H\tau_{yy})}{\partial y} \right) + F_{cy} + F_{wy} \quad (6)$$

Where  $g$  is the acceleration of gravity ( $m/s^2$ );  $n$  is the Manning coefficient;  $|\vec{q}|$  is the specific flow module ( $m^2/s$ );  $\rho$  is the density of water ( $kg/m^3$ );  $F_{cx}$  and  $F_{cy}$  are the components of the Coriolis Force (N); and  $F_{wx}$  and  $F_{wy}$  the components of the force due to the wind (N);  $\tau_{ij}$  is the Reynolds tensor ( $N/m^2$ ) (Eq. 7).

$$\tau_{ij} = \nu \left( \frac{\partial \bar{U}_i}{\partial x_j} + \frac{\partial \bar{U}_j}{\partial x_i} \right) \quad (7)$$

Where  $\bar{U}_i$  is the component of the average velocity in the direction  $i$  ( $m/s$ );  $\nu$  is the kinematic viscosity. The turbulence model is the length of mixture, which takes into account the distance from the wall from which the size of the turbulent structures is no longer influenced by the wall (Rodi, 1993). In this case, the turbulent viscosity is calculated by Eq. 8.

$$\nu_t = L_m^2 \sqrt{2D_{ij}D_{ij}} \quad (8)$$

Where  $D_{ij}$  (Eq. 9) is the tensor of the deformation rate of the average movement.

$$D_{ij} = \frac{1}{2} \left( \frac{\partial \bar{U}_i}{\partial x_j} + \frac{\partial \bar{U}_j}{\partial x_i} \right) \quad (9)$$

The hydrodynamic regime considered in this study was the stationary one, which is a good hypothesis, considering that the water levels and streamflow of the analyzed São Marcos river section are controlled by the operation maneuvers of HPP Serra do Facão. The influence of the wind is not considered, as the study area is located in the central region of Brazil, and, in this case, the air currents were neglected. The Coriolis Force effect is neglected because the study domain is small.

## 2.4 Software H2D2

The *H2D2* software (GRE-EHN, 2018) is composed of pre and post finite element processors. The program performs all stages of integration of the various field data for the design of the Terrain Elevation Model (TEM) supported by a Finite Element mesh. Also, using the Finite Element Method (FEM), hydrodynamic simulations are performed based on Saint-Venant's equations. *H2D2* was developed by the Research and Studies Group on Numerical Eco-Hydraulics (GRE-EHN) of INRS-ETE of the University of Quebec - Canada. Some studies have demonstrated the potential for application of the *H2D2* model (Blanco *et al.*, 2013; Holanda *et al.*, 2017).

The model is two-dimensional-longitudinal-transversal. The conservation equations for mass and momentum are integrated into the depth. In this way, the values obtained for the velocities are average in the vertical direction. The *FEM* makes a quadratic interpolation in each element of the triangular mesh, this means that the mesh is formed by triangles consisting of six nodes, called *T6* (Figura 3). Thus, the *FEM* allows not only to represent the average values in a variable field, but also to solve the continuum mechanics equations applicable to the analyzed physical problem. In Figure 3, the variables  $h$  (water height),  $H$  (depth),  $z_f$  (bottom dimension) and the roughness coefficient (points 1, 3, 6) are linearly interpolated, as their gradients are less accentuated than the gradients of velocities and specific flows (points 2, 4, 5), which are quadratically interpolated, as they generally have more pronounced gradients.

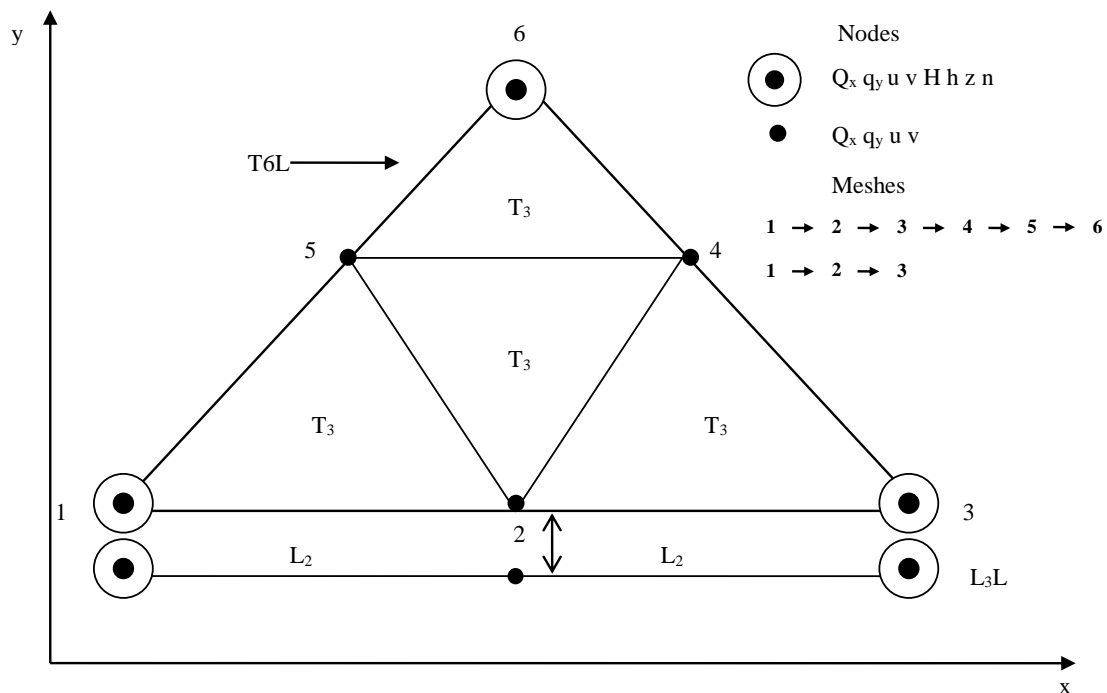


Figure 3. H2D2 triangularization.  
Source: Secretan *et al.* (2001).

Thus, *H2D2* generates the finite element mesh, which stores all the input quantities necessary to solve the Saint-Venant equations, as well as the quantities resulting from the simulation of the two-dimensional flow (velocities in  $x$  and  $y$ , depth and water level). The input quantities considered in the model are: the  $x$ ,  $y$  and  $z$  coordinates, interpolated via *MEF* and transferred to the hydrodynamic mesh, the Manning coefficient and the boundary conditions. The mesh is generated from a frontal isotropic algorithm, which uses a single spacing parameter and tries to generate the most regular triangles (Secretan *et al.*, 2000).

## 2.5 Quasi 3D model

The Quasi 3D model aims to simplify a 3D simulation based on the results of 2DH hydrodynamic simulations, as these require less computational time. Luijendijk *et al.* (2010) observed that Quasi 3D modeling is computationally efficient, since it adds only about 15-20% to the execution time of a 2DH simulation, which is less compared to an increase in the execution time of 250-800% when using a 3D simulation.

According to Martin and McCutcheon (1998) the velocity on the surface of a river or channel can be estimated through a logarithmic distribution, where the velocity on the surface is equal to 6/5 of the average vertical velocity. The maximum velocity, on the surface, is 6/5 of the average vertical velocity. The development of velocity as a function of depth occurs in a logarithmic way (Figure 4).

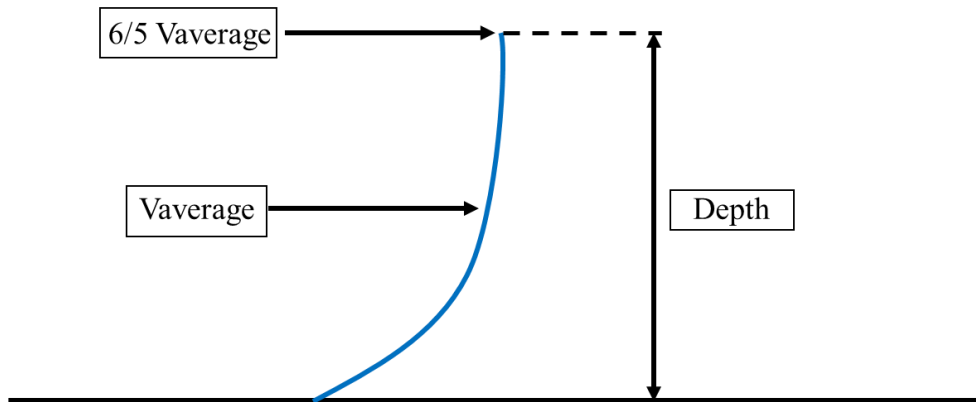


Figure 4. Conditions for the projections of the velocities of the Quasi 3D model.

The calculations to determine the velocity results for a single point are given as follows:

- The maximum velocity, on the surface, is 6/5 of the average vertical velocity;
- The admitted velocity at the bottom of the channel is 0.001 m/s, of which the adopted depth is 0.001 m due to the non-slip condition limited to a value other than 0 (zero) due to the logarithmic function adopted for the calculations of this work. Through Eq. 10, the logarithmic distribution of velocities is determined.

$$vel(z) = A \cdot \ln(z) + B \quad (10)$$

Where  $vel(z)$  is the velocity (m/s) and  $z$  is the depth (m).

The values of  $A$  and  $B$  in Eq. 10 can be determined by choosing two points from the three points, of which velocity and depth are known (Figure 4).

The generation of the Quasi 3D profile of a cross section starts from the results of the 2D hydrodynamic simulations, i.e., the isosurfaces of velocity and depth, which support the generation of a section of interest. From points in this section, depth and average velocity data are extracted for the Quasi 3D profile.

## 2.6 Hydraulic Power Estimation

The velocity and depth of rivers is a parameter that allows the dimensioning of the rotor diameter in a hydrokinetic turbine design (Punys *et al.*, 2015). According to Kumar and Sarkar (2016), the output power of the turbine is affected mainly by three factors: velocity, turbine rotor area, and efficiency of the energy conversion system (Eq. 11).

$$P = \frac{1}{2} \rho A U^3 C_p \quad (11)$$

Where  $P$  is the hydraulic power (W),  $\rho$  is the density of the water ( $kg/m^3$ ),  $A$  is the area swept by the rotor blades ( $m^2$ ),  $U$  is the water velocity (m/s) and  $C_p$  is the power coefficient (Betz coefficient).

According to Yuce and Muratoglu (2015), the maximum efficiency that an ideal turbine can attain is known as the Betz limit. Betz's law proposes that the theoretical maximum power coefficient for a rotating turbine in fluid flow is 0.593. However, according to Vermaak *et al.* (2014), the small turbines have reducing the power coefficient to 0.25. The diameter of the rotor is needed to calculate the swept area. Considering the submersion of the turbine, the suggestion of Kolekar and Banerjee (2015) was considered. In this case, the end of the rotor must be within a radius of the solid surface of the river and a half radius of the free surface.

### 3. RESULTS

#### 3.1 Hydrodynamic Mesh

Due to the unavailability of bathymetry data from the downstream reservoir of *HPP* Serra do Facão, topobathimetric data were extracted from satellite images, according to the previously mentioned method. Thus, bathymetry points were extracted from the area of interest, using an image (.tif). Figure 5 shows the hydrodynamic mesh in triangular Finite Elements of the Serra do Facão *HPP* downstream reservoir projected in a satellite image of the region. The *X* and *Y* coordinates of the bathymetry and topography data are georeferenced in *UTM* coordinates, in *WGS84* zone 23*S* so that the *H2D2* platform (GRE-EHN 2020) can perform hydrodynamic simulations with these data.

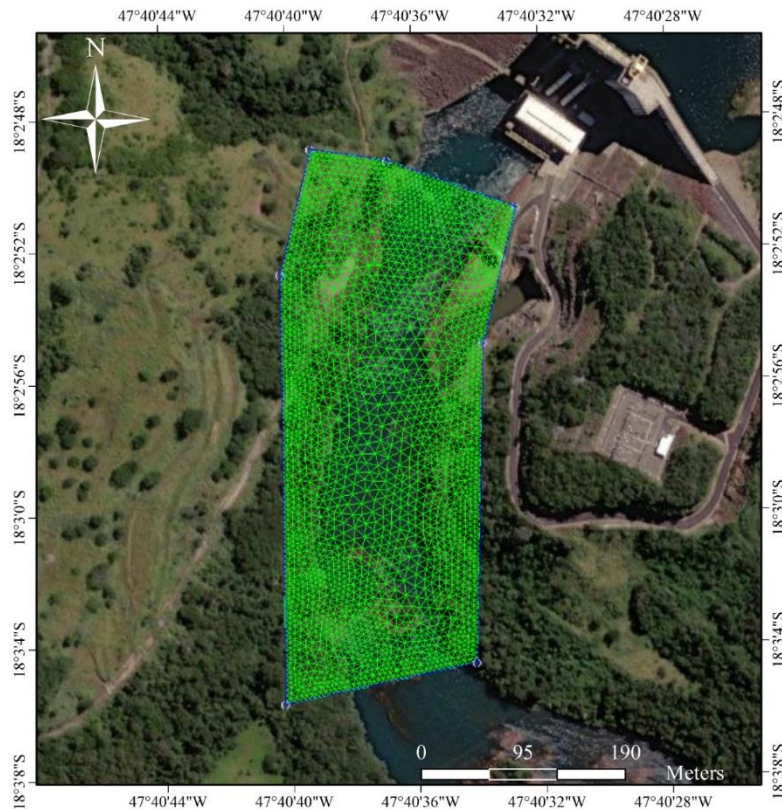


Figure 5. Mesh with refinement of 5 meters, 4,092 triangular finite elements and 8,449 nodes.

#### 3.2 Streamflow simulation of the Serra do Facão HPP downstream reservoir

A simulation was carried out using the level-level condition, for the *Max Maximorum* level downstream from HPP Serra do Facão (SEFAC, 2020), i.e.,  $NA = 680.6$  m. The simulated streamflow was  $465$  m<sup>3</sup>/s with a maximum velocity of  $2.5$  m/s. This velocity refers to the Quasi 3D model (Figure 9). Figures 5 and 6 show the isosurfaces of velocity and depth, respectively, of the simulation carried out and projected in a satellite image of the downstream reservoir of HPP Serra do Facão.

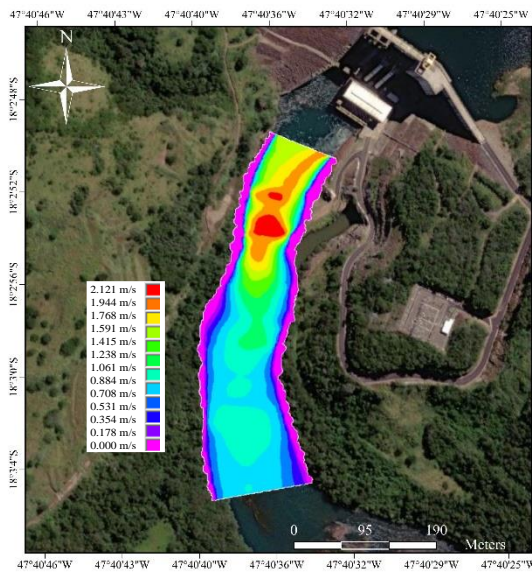


Figure 5 – Velocity isosurfaces.

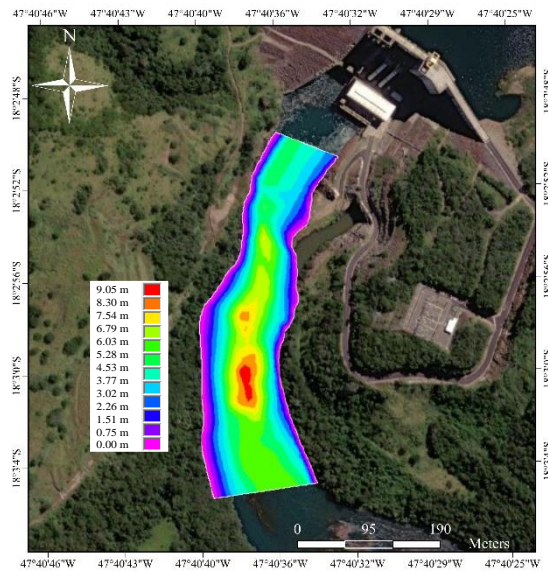


Figure 6 - Depth isosurfaces.

Figure 7 shows the simulated transect in the higher velocity regions of Figure 5.

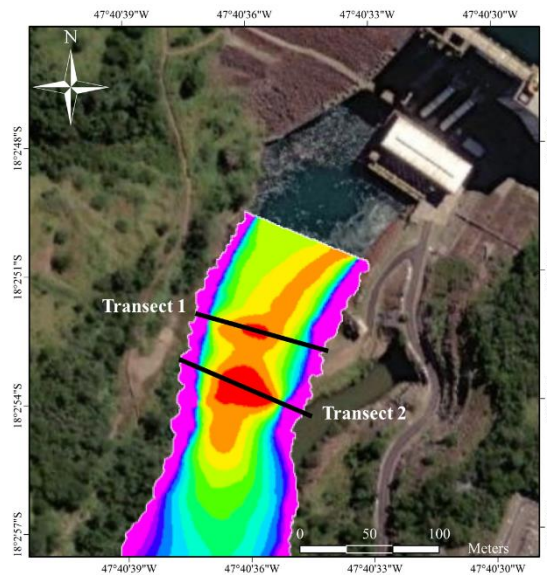


Figure 7 - Regions of maximum velocity and simulated transect in the downstream reservoir of HPP Serra do Facão.

Figures 8 and 9 show, respectively, the velocity profiles in the transects 1 and 2. In the transect 1 (Figure 8), the maximum velocity is approximately equal to  $2.5 \text{ m/s}$  and in the transect 2 (Figure 9), this velocity is reached. Considering the maximum velocities and depths shown in Figures 6 and 7, the hydraulic power of two turbines (one for each transect) was determined using Eq. 11, with  $\rho = 1000 \text{ kg/m}^3$ ,  $A = 4.91 \text{ m}^2$  (diameter of  $2.5 \text{ m}$ ),  $U = 2.5 \text{ m/s}$  and  $C_p = 0.25$ , with  $P = 19.2 \text{ kW}$ . Holanda *et al.* (2017) evaluated the hydrokinetic potential of the downstream reservoir of the Tucuruí HPP, in the state of Pará, Brazil and projected the implementation of 10 hydrokinetic turbines, producing  $2.04 \text{ GWh/year}$ . The power to generate this energy is much greater than the power determined in the present study, but it is noteworthy that in the work of Holanda *et al.* (2017) turbines with a diameter of  $10 \text{ m}$  were designed. Santos *et al.* (2021) designed on the Jamari River, in the state of Rondônia, Brazil, a hydrokinetic arrangement of three turbines, with diameters of  $4 \text{ m}$  and a maximum velocity of  $1.75 \text{ m/s}$ . In this case, the total hydraulic power of the arrangement is  $25.94 \text{ kW}$  comparable to the power determined for the two turbines analyzed in the present work.

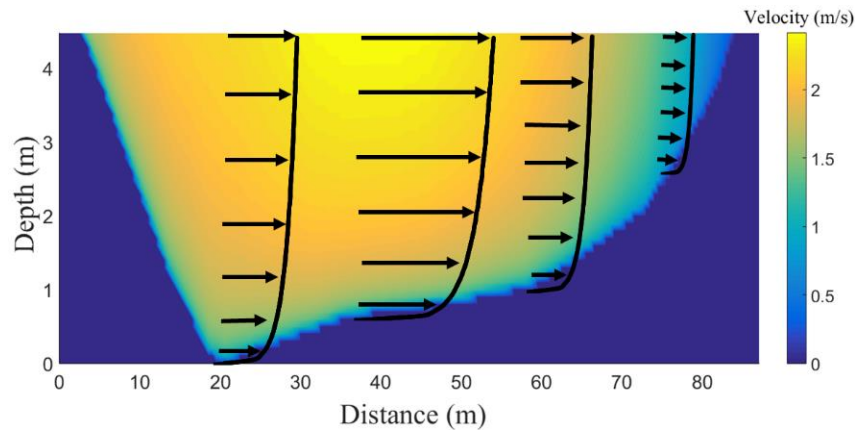


Figure 8 - Velocities in the cross section of transect 1 in the downstream reservoir of HPP Serra do Facão.

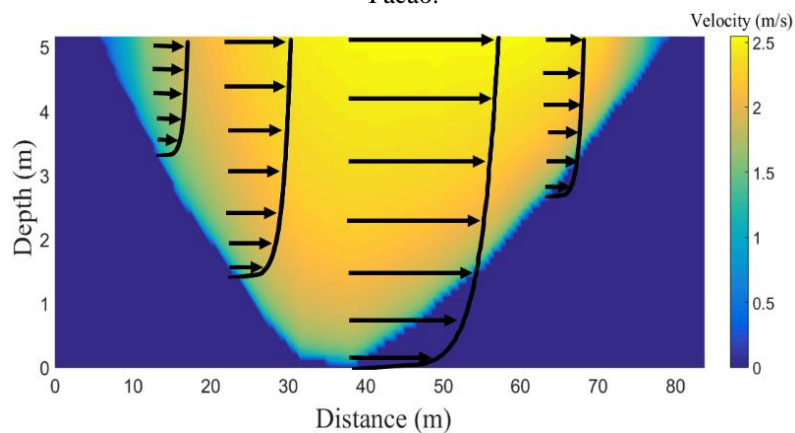


Figure 9 - Velocities in the cross section of transect 2 in the downstream reservoir of HPP Serra do Facão.

#### 4. CONCLUSION

The presented methodology was able to extrapolate  $2DH$  velocities to the  $3D$  domain through a Quasi  $3D$  model in an HPP downstream reservoir. In this case, the bathymetry and topography data were extracted from satellite images and proved to be capable of representing the downstream channel of the Serra do Facão HPP reservoir, Goiás, Brazil. The regions of velocity isosurfaces resulting from  $2DH$  modeling were selected due to the higher velocities, which maximize the generation of hydrokinetic energy. Thus, for two cross sections with higher velocities and maximum depths of  $5\text{ m}$ , the maximum simulated velocity by model Quasi  $3D$  was equal to  $2.5\text{ m/s}$ . With this velocity and taking half the depth to dimension the diameter of two hydrokinetic turbines, one for each section, a hydraulic power equal to  $19.2\text{ kW}$  was calculated. This result is interesting, as hydrokinetic parks can be installed in the downstream reservoirs, increasing the potential found in the study.

#### 5. ACKNOWLEDGEMENTS

The authors would like to thank Serra do Facão Energia S.A. for providing financial support for the development of the project (ANEEL:P&D06899-2002/2020) - Desenvolvimento de metodologia para determinação de potencial de energia hidrocinética em usinas hidroelétricas. The authors would like to thank the CAPES - Finance Code 001.

#### 6. REFERENCES

- Blanco, C.J.C., Sena, M.J.S., Amarante Mesquita, A. L., Furtado Filho, M. D. C., and Secretan, Y., 2013. "Hydrodynamic evaluation of a flood embankment in the Amazon estuary region- Brazil". *Proceedings of the Institution of Civil Engineers*. Civil Engineering, Vol. 166, pp. 49-55.
- Dos Santos, I.F.S., Camacho, R.G.R., and Tiago Filho, G.L. 2021, "Study of the wake characteristics and turbines configuration of a hydrokinetic farm in an Amazonian river using experimental data and CFD tools". *Journal of Cleaner Production*, Vol. 299, p. 126881.

- Duvoy, P., and Toniolo, H., 2012. "HYDROKAL: A module for in-stream hydrokinetic resource assessment". *Computers & Geosciences*, Vol. 39, pp. 171-181.
- FURNAS, 2020, *Plataforma FURNAS, Electricity Generation, Transmission and Sale* (in Portuguese), <https://www.furnas.com.br/serradofacao/?culture=pt>. Accessed 10 August 2020.
- Geyman, E.C., and Maloof, A.C, 2019. "A simple method for extracting water depth from multispectral satellite imagery in regions of variable bottom type". *Earth and Space Science*, Vol. 6, pp. 527–537.
- GRE-EHN, 2018, *Numerical Eco-Hydraulic Research and Studies Group*, <https://www.gre-ehn.ete.inrs.ca/H2D2>, Accessed 16 January 2018.
- Heniche, M.A., Secretan, Y., Boudreau, P., and Leclerc, M., 2000. "A two-dimensional finite element drying-wetting shallow water model for rivers and estuaries". *Advances Water Resources*, Vol. 23, pp. 359-372.
- Guerra, M., and Thomson, J., 2019. "Wake measurements from a hydrokinetic river turbine". *Renewable Energy*, Vol. 139, pp. 483-495.
- Holanda, P. S., Blanco, C.J.C., Mesquita, A.L.A., Brasil Junior, A.C.P., Figueiredo, N.M., Macedo, E.N., and Secretan, Y., 2017. "Assessment of hydrokinetic energy resources downstream of hydropower plants". *Renewable Energy*, Vol. 217, pp. 1203-1214.
- IBGE, 2020, *Instituto Brasileiro de Geografia e Estatística* (in Portuguese), <http://www.ibge.gov.br/home>. Accessed 15 August 2020.
- Kerr, J.M., and Purkis, S., 2018. "An algorithm for optically-deriving water depth from multispectral imagery in coral reef landscapes in the absence of ground-truth data". *Remote Sensing of Environment*, Vol. 210, pp. 307–324.
- Kolekar, N., and Banerjee, A., 2015. "Performance characterization and placement of a marine hydrokinetic turbine in a tidal channel under boundary proximity and blockage effects". *Applied Energy*, Vol. 148, No. 1, pp. 121-133.
- Lee, Z., Carder, K.L., Mobley, C.D., Steward, R.G., and Patch, J.S., 1999. "Hyperspectral remote sensing for shallow waters: 2. Deriving bottom depths and water properties by optimization". *Applied Optics*, Vol. 38, No. 18, pp. 3831–3843.
- Luijendijk, A., Henrotte, J., Walstra, D.J.R., and VAN ORMONDT, M., 2010. "QUASI 3D Modelling of surf zone dynamics". In *Proceedings of the 32nd International Conference on Coastal Engineering, ICCE 2010*, June/July, Shanghai, 2010.
- Kumar, D., and Sarkar, S., 2016. "A review on the technology, performance, design optimization, reliability, techno-economics and environmental impacts of hydrokinetic energy conversion systems". *Renewable and Sustainable Energy Reviews*, Vol. 58, pp. 796-813.
- Martin, J.L., and Mc Cutcheon, S.C., 1998. *Hydrodynamics and Transport for Water Quality Modeling*. Editora aylor & Francis, Boca Raton - London - New York.
- ONS, 2020. National Electric System Operator (in portuguese), <http://www.ons.org.br/>. Accessed 25 August 2020.
- Puny, P., Adamonyte, I., Kvaraciejus, A., Martinaitis, E., Vyciene, G., and Kasiulis, E., 2015. "Riverine hydrokinetic resource assessment. A case study of a lowland river in Lithuania". *Renewable and Sustainable Energy Reviews*, Vol. 50, pp. 643-652.
- Saint-Venant, A.J.C., 1871. "Théorie du mouvement non-permanent des eaux, avec application aux crues des rivières et à l'introduction des marées dans leur lit". *C. R. Acad. Sc. Paris*, Vol. 73, pp. 147-154.
- SEFAC, 2020. *Serra do Facão Energy S.A* (in Portuguese), <https://sefac.com.br/empresa/nossa-historia/>. Accessed 08 August 2020.
- Secretan, Y., Leclerc, M., Duschesne, S., and Heniche, M., 2001. "Une méthodologie de modélisation numérique de terrain pour la simulation hydrodynamique bidimensionnelle" *Revue des Sciences de l'eau*, Vol. 14, pp. 187-212.
- Secretan, Y., Leclerc, M., 1998. "Modeleur a 2D hydrodynamic GIS and simulation software". In: *Proceedings of the Hydroinformatics-98*, pp 1-18, Copenhagen, Denmark.
- Secretan, Y., Roy, Y., Granger, Y., and Leclerc, M., 2000. *Modeleur 1.0a07 – Guide d'utilisation* (in French). Rapport R482-G3F, INRS-EAU, Québec, CA.
- Stumpf, R.P., Holderied, K., and Sinclair, M., 2003. "Determination of water depth with high-resolution satellite imagery over variable bottom types". *Limnology and Oceanography*, Vol. 48, No. 1, pp. 547–556.
- Ramirez, M.R., Cuervo, F.I., Rico, C.A.M., 2016. "Technical and financial valuation of hydrokinetic power in the discharge channels of large hydropower plants in Colombia: A case study". *Renewable Energy*, Vol. 99, pp.136-147.
- Vermaak, H.J., Kusakana, K., and Koko, S.P., 2014. "Status of micro-hydrokinetic river technology in rural applications: A review of literature". *Renewable and Sustainable Energy Reviews*, Vo. 29, pp. 625-633.
- Yuce, M.I., and Muratoglu, A., 2015. "Hydrokinetic energy conversion systems: A technology status review". *Renewable and Sustainable Energy Reviews*, Vol. 43, No. 3, pp. 72-82.

## 7. RESPONSIBILITY NOTICE

The author(s) is (are) the only responsible for the printed material included in this paper.